Replacing Ag TS SCH 2 -R with Ag TS O 2 C-R in EGaIn-Based Tunneling Junctions Does Not Significantly Change Rates of Charge Transport

Replacing $Ag^{TS}SCH_2$–R with $Ag^{TS}O_2C$–R in EGaIn-Based Tunneling Junctions Does Not Significantly Change Rates of Charge Transport

Kung-Ching Liao,[1] Hyo Jae Yoon,[1] Carleen M. Bowers,[1] Felice C. Simeone,[1] and George M. Whitesides[1,2,3*]

[1]Department of Chemistry and Chemical Biology, Harvard University, 12 Oxford Street, Cambridge, Massachusetts 02138 United States,

[2]Wyss Institute for Biologically Inspired Engineering, Harvard University, 60 Oxford Street, Cambridge, Massachusetts 02138 United States, and

[3]Kavli Institute for Bionano Science & Technology, Harvard University, 29 Oxford Street, Massachusetts 02138 United States

*Corresponding author, email: gwhitesides@gmwgroup.harvard.edu

Abstract:

This paper compares rates of charge transport by tunneling across junctions with the structures $Ag^{TS}X(CH_2)_{2n}CH_3//Ga_2O_3/EGaIn$ (n = 1 – 8 and X = $–SCH_2–$ and $–O_2C–$); here Ag^{TS} was template-stripped silver, and EGaIn is the eutectic alloy of gallium and indium. Its objective was to compare the tunneling decay coefficient (β, $Å^{-1}$) and the injection current (J_0, A/cm^2) of the junctions comprising SAMs of *n*-alkanethiolates and *n*-alkanoates. Replacing $Ag^{TS}SCH_2–R$ with $Ag^{TS}O_2C–R$ (R = alkyl chains) had no significant influence on the value of J_0 (*ca.* 3×10^3 A/cm^2) or on the value of β (0.75 – 0.79 $Å^{-1}$); an indication that such changes (both structural and electronic) in the $Ag^{TS}XR$ interface do not influence the rate of charge transport. A comparison of junctions comprising oligo(phenylene)carboxylates and *n*-alkanoates showed, as expected, that the value of β for aliphatic (0.79 $Å^{-1}$) and aromatic (0.60 $Å^{-1}$) SAMs differed significantly.

Studies of charge tunneling through self-assembled monolayer (SAM)-based junctions have focused predominately on the influence of backbone substituents[1-4] or terminal functional groups[5-8] on rates of charge transport. The effect of changing the group (which we call the "anchoring group") that links the SAM to the metal substrate has not been explored in detail;[9, 10] only a few studies have approached this issue at the single-molecular level using scanning tunneling microscopy[11-14] or conducting atomic force microscopy.[15-17] Here we explore the replacement of the anchoring group using a large-area (50 μm^2 on average) SAM-based junction having the structure Ag^{TS}–X–$(CH_2)_{2n}CH_3$//Ga_2O_3/EGaIn,[18, 19] where X is the anchoring group for the SAM; Ag^{TS} is a template-stripped silver substrate;[20] EGaIn is a liquid metal, eutectic gallium–indium alloy; and Ga_2O_3 is a thin semiconducting film that forms spontaneously on the surface of EGaIn in air.[18] We prepared analogous junctions, compositionally different only in the replacement of $Ag^{TS}SCH_2$–R with $Ag^{TS}O_2C$–R, and compared the rates of charge transport by tunneling through these two junctions. The similarity in these rates establishes that the rate of charge transport across the SAM-based tunneling junction is surprisingly insensitive to changes in the composition of the interface between the Ag^{TS} and the SAM.

While the study of organothiolates in molecular electronics is limited by the availability and stability of thiols, a large variety of carboxylic acids are commercially available, or easily accessible by straightforward synthetic routes. The ability to study charge transport through junctions of the structure $Ag^{TS}O_2CR$//Ga_2O_3/EGaIn makes mechanistic studies of tunneling more accessible experimentally, and provides a new system that helps to clarify the role of the interfaces to electrodes in tunneling junctions.

Background. The rate of charge transport by tunneling through SAMs decays exponentially with increasing distance between the top and bottom electrodes. In studies analogous to those in

many other systems, we determined that junctions of the structure $Ag^{TS}SCH_2–(CH_2)_{2n}CH_3//Ga_2O_3/EGaIn$ (across a range of molecular lengths and structures) obey the simplified Simmons equation (1),[21-24] where J (A/cm^2) is the measured current density; β (Å^{-1}) is the tunneling decay coefficient; we take d (Å) to be the extended length of molecule. The injection current, J_0, represents the current density when $d = 0$; that is, the value of J for a

$$J = J_0 e^{-\beta d} \quad (1)$$

hypothetical system consisting only of the top and bottom electrodes, and the metal–SAM interfaces.[24] Values of β characterize tunneling junctions having a range of alkyl structures are similar; values of J_0 vary among different types of junctions, for reasons that are at least partially understood.[19]

In an electrode–SAM–electrode junction, charge crosses a tunneling barrier whose energetic topography is not exactly known, but which describes the space (including the SAM, the interfaces between the SAMs and the electrodes, and any surface films on the electrodes) between the two metallic junctions. In principle, one approach to manipulating the shape of the tunneling barrier, and thus to influencing the rate of charge transport, is to introduce functional groups into the structure of the SAM that are capable of influencing this topography, and thus the rate or mechanism of charge transport.[25-29] Using Ga_2O_3/EGaIn top-electrodes, however, we found previously that the tunneling current is insensitive to the incorporation of several functional groups familiar in organic chemistry[4, 8] (e.g., an amide, –CONH– or –NHCO–) in the backbone of the molecules in the SAM, or a variety of functional groups (both aliphatic and aromatic) that are not electrochemically active at the terminus of the SAM ostensibly in contact with the Ga_2O_3 film.[8]

Most studies using EGaIn-based tunneling junctions have focused on SAMs of *n*-alkanethiolates on Au or Ag. This focus on systems based on the Ag–SR anchoring group has limited our understanding of the role of the interface between the Ag (or Au) and the SAM to a single chemical and electronic structure. Here, we replaced *n*-alkanethiolates with *n*-alkanoates in order to examine the effect of the bottom-interface on the value of J_0 for a Ag^{TS}–SAM//Ga_2O_3/EGaIn junction. *n*-Alkanoic acids form highly-ordered monolayers on metal surfaces;[30] in particular, monolayers composed of long-chain *n*-alkanoates on Ag exhibit nearly crystalline packing of the hydrocarbon backbone, all-*trans* methylene conformations, and a bidentate ionic binding coordination of the carboxylate to the surface.[30-33] Previous reports[31, 33] showed that the carboxylate moiety coordinates through ionic interactions with the surface of the Ag, and a native oxide of Ag possibly (or in our view probably) exists at the interface between the metal and the carboxylate. SAMs of *n*-alkanethiolates on Ag(111) have a $(\sqrt{7} \times \sqrt{7})R10.9^{o}$ cell with 4.4 Å nearest neighbor spacing.[34] The structure of *n*-alkanoate SAMs on Ag is comparable to that of *n*-alkanethiolates; the tilt angle of the alkyl chains is $15 - 25^{o}$ (from the surface normal), and they form a *p*(2x2) overlayer with a lattice spacing of 5.8 Å, indicating a densely packed monolayer,[34, 36] as summarized in Table S1 (see the supplementary information).

Results and discussion

Preparation of SAMs. We prepared SAMs with commercially available *n*-alkanoic acids, $CH_3(CH_2)_{2n}CO_2H$ where n = 1 – 8 (i.e., the number of methylene groups). The preparation of *n*-alkanoate SAMs on Ag^{TS} followed previously reported literature procedures.[30, 35] Freshly prepared Ag^{TS} substrates were introduced into a solution of 1 mM *n*-alkanoic acid in anhydrous *n*-hexadecane for 3 hr. After incubation at ambient conditions, we rinsed the SAM-bound Ag substrates three times with anhydrous hexane and dried the substrates under a gentle stream of

nitrogen. We characterized the surface of SAMs of *n*-alkanoates on Ag^{TS} using contact angle measurements. The monolayers exhibited low wettability: static contact angles for wetting by water and *n*-hexadecane were 113 ± 7^o and 45± 3^o, respectively. These values are consistent with previous reports by Tao *et al.*[30] and Lin *et al.*[32]

Measurements of Tunneling Currents. We measured *J(V)* for junctions of the form $Ag^{TS}O_2C–(CH_2)_{2n}CH_3//Ga_2O_3/EGaIn$ over the range of ±0.5 V as a function of the length of alkyl chain (n = 1 – 8); we did not observe rectification of current (Figure 1b). Each curve of log|*J(V)*|*versus V* was generated with 430 – 720 data from at least 20 different junctions on three to four samples, and the yield of working junctions was ≥ 84% (Table 1). As observed in many previous studies, the binned *J* values (100 bins in the range of log|*J*| = -6 to 4, with units of A/cm^2; the width of each bin is log|*J*|~0.1) had a distribution that was approximately log-normal; this form justified fitting each histogram of log|*J*| with a Gaussian curve. From these fittings, we obtained mean values of log|*J*| ($\log|J|_{mean}$) and standard deviations (σ_{log}) of the corresponding Gaussian fits (Figure 2); $\log|J|_{mean}$ is indistinguishable from the log median value ($\log|J|_{median}$) of log|*J*| determined in each histogram (Table 1). Values of σ_{log} ranged from 0.1 to 0.5; these values are similar to those observed in the junctions of *n*-alkanethiolate SAMs.[36] As expected from the simplified Simmons equation, the rate of charge transport across junctions containing SAMs of *n*-alkanoates followed an exponential decrease with increasing length of the *n*-alkyl groups (n=1 to 8 for $CH_3(CH_2)_{2n}CO_2$). Figure 1c shows a plot of log|*J*| *versus* calculated length (Å) which includes the length of terminal H–C bond but excludes the length of Ag–O bond, which we considered to be a part of the Ag^{TS}–SAM interface (in this view $[O_2]C(CH_2)_{2n}CH_3$ and $[S]CH_2(CH_2)_{2n}CH_3$ are compatible structure). The linear-least square fit of the full set of data ($CH_3(CH_2)_{2n}CO_2H$, n = 1 – 8) yielded the log-injection current, $\log|J_0| = 3.5 \pm 0.2$ A/cm^2

(coefficient of determination, $R^2 = 0.99$). The slope derived from the plot of ln|*J*| *versus* the length of molecules provided the tunneling decay coefficient, $\beta = 0.79 \pm 0.02$ Å^{-1}.

Comparisons of *J*(V) data from *n*-alkanoate and *n*-alkanethiolate[36] SAMs on Ag (Table 1) indicate that these junctions have a statistically indistinguishable tunneling decay coefficient ($\beta = 0.79 \pm 0.02$ Å^{-1} for *n*-alkanoates; $\beta = 0.75 \pm 0.02$ Å^{-1} for *n*-alkanethiolates, both with even numbers of carbon atoms) and injection current ($\log|J_0| = 3.5 \pm 0.2$ A/cm^2 derived from *n*-alkanoates; $\log|J_0| = 3.2 \pm 0.3$ A/cm^2 derived from *n*-alkanethiolates). The similarities in β and J_0 imply that any difference in the contribution of the Ag-thiolate and the Ag-oxygen interface to the shape of the tunneling barrier is not detectable by our methods, although these two interfaces are chemically and electronically quite different. We conclude therefore, that the Ag^{TS}–X–R interface does not contribute to the features of the tunneling barrier that influence tunneling current. While we and Tao *et al*. have not yet defined whether mono- or multi-layers of native silver oxide are sandwiched between the Ag metal and the carboxylate, the *J*–*V* measurements suggest that this film, if any, is conductive, and makes no contribution to the resistance of the junction.

Several studies have predicted or reported a distinct electronic influence from different metal-molecule interfaces used in junction measurements.[11, 37-40] For example, Zimbovskaya and Pederson[41] examined different metal-molecule interfaces theoretically, and concluded that different modes of binding at the interfaces might influence the conductance of junctions. Chu *et al*.[42] reported that the current through molecules with an Au–amine junction is larger by a factor of 10 than that with an Au–thiolate linkage, and attributed this observation to the difference of the electronic interactions between the gold and the anchoring group. Our findings, however, indicate that replacing $AgSCH_2$–R with AgO_2C–R (a large change in the structure of the bottom

metal–SAM interface) has no significant influence on the rates of charge transport across *n*-alkyl-based SAMs.

Junctions comprising SAMs of aromatics. Tao and coworkers reported the formation and characterization of SAMs of biphenyl-4-carboxylic acid[43] and *p*-terphenyl-4-carboxylic acid[33] on Ag. Their report showed that the oligo(phenylene)carboxylate binds perpendicularly (from the surface normal) through a symmetric ionic coordination to the surface of Ag.[43] We incorporated SAMs of oligo(phenylene)carboxylic acids into junctions of the structure $Ag^{TS}O_2C(C_6H_4)_nH//Ga_2O_3/EGaIn$ (n = 1 – 3) and characterized rates of charge transport across them (Figure 3a; Table 2). Figure 4 shows the histograms of log|*J*| at -0.5 V and relative Gaussian fittings for benzoic acid, biphenyl-4-carboxylic acid, and *p*-terphenyl-4-carboxylic acid. We found a narrow distribution of current density with a small range of σ_{log} (0.2 – 0.3) for each SAM. The value of log|J_0| (3.0 ± 0.2 A/cm^2) of the $Ag^{TS}O_2C(C_6H_4)_nH//Ga_2O_3/EGaIn$ junctions was estimated from a linear least squares fit (R^2 = 0.98) of the plot of log|*J*| *versus* the calculated length of the molecules (Å); β was 0.60 ± 0.2 Å^{-1}.

The tunneling decay coefficient of *n*-alkanoate-based SAMs (0.79 Å^{-1}) is higher than that of oligophenylene-containing SAM (0.60 Å^{-1}), and suggests (as have other studies[10, 29, 44, 45]) that in these oligophenylene-based SAMs i) the shape of the tunneling barrier is influenced both by the width of the tunneling barrier and the electronic structure of the molecules forming the SAM; ii) charge transport by tunneling through poly-aromatic SAMs is more rapid than through non-conjugated SAMs (a conclusion in agreement with a number of other studies). The value of log|J_0|, derived from the junctions comprising SAMs of oligophenylene carboxylates (log|J_0| = 3.0 ± 0.2 A/cm^2), is indistinguishable to that of *n*-alkanoates (log|J_0| = 3.5 ± 0.2 A/cm^2) at the precision of our measurements.

Conclusion

Within the constraints of the accuracy and uncertainties of our system, the Ag–SAM interface has no significant influence on the rates of tunneling across an *n*-alkane-based tunneling barrier, since the tunneling currents through junctions of *n*-alkanoate and of *n*-alkanethiolate SAMs are indistinguishable in our experiments. Although the details of the bonds at the $Ag^{TS}O_2C$–R interface are quite different from those at the $Ag^{TS}SCH_2$–R interface,[31, 33] this study suggests that nature of the coordination between the metal of bottom electrode (Ag^{TS}) and the SAM does not significantly influence the rate of tunneling. The tunneling decay coefficient for *n*-alkanoates and for *n*-alkanethiolates on silver are indistinguishable (0.75–0.79 $Å^{-1}$), and are similar to previous literature reports for junctions with different structures.[19, 46-48] The coefficient for oligophenylene carboxylates (β = 0.60 $Å^{-1}$) is, as expected from prior work, significantly lower than that of alkyl-based SAMs.

We conclude that the $Ag^{TS}O_2CR//Ga_2O_3$/EGaIn junction provides a versatile and convenient experimental system with which to investigate factors that may influence rates of charge transport through SAM-based junctions, and to understand the mechanisms underlying these influences. The use of carboxylate anchoring groups promises to simplify the study of tunneling junctions greatly by eliminating the instability (due to oxidation, desulfurization, and other processes) and multiple chemical incompatibilities of the commonly-studied structures based on organic thiolates. Moreover, carboxylates are more flexible than thiols from the vantage of physical-organic studies, because they are commercially available, stable (especially to oxidation), and easily handled and purified.

Methods

See the Supplementary Information for the materials, sample preparations, and procedures for measurements of tunneling.

References

1. Wold, D.J., Haag, R., Rampi, M.A. & Frisbie, C.D. Distance Dependence of Electron Tunneling through Self-Assembled Monolayers Measured by Conducting Probe Atomic Force Microscopy: Unsaturated versus Saturated Molecular Junctions. *J. Phys. Chem. B* **106**, 2813-2816 (2002).
2. Pobelov, I.V., Li, Z. & Wandlowski, T. Electrolyte Gating in Redox-Active Tunneling Junctions: An Electrochemical STM Approach. *J. Am. Chem. Soc.* **130**, 16045-16054 (2008).
3. Fracasso, D., Valkenier, H., Hummelen, J.C., Solomon, G.C. & Chiechi, R.C. Evidence for Quantum Interference in SAMs of Arylethynylene Thiolates in Tunneling Junctions with Eutectic Ga–In (EGaIn) Top-Contacts. *J. Am. Chem. Soc.* **133**, 9556-9563 (2011).
4. Thuo, M.M. *et al.* Replacing $-CH_2CH_2-$ with $-CONH-$ Does Not Significantly Change Rates of Charge Transport through Ag^{TS}-SAM//Ga_2O_3/EGaIn Junctions. *J. Am. Chem. Soc.* **134**, 10876-10884 (2012).
5. Wassel, R.A., Credo, G.M., Fuierer, R.R., Feldheim, D.L. & Gorman, C.B. Attenuating Negative Differential Resistance in an Electroactive Self-Assembled Monolayer-Based Junction. *J. Am. Chem. Soc.* **126**, 295-300 (2003).
6. Engelkes, V.B., Beebe, J.M. & Frisbie, C.D. Length-Dependent Transport in Molecular Junctions Based on SAMs of Alkanethiols and Alkanedithiols: Effect of Metal Work Function and Applied Bias on Tunneling Efficiency and Contact Resistance. *J. Am. Chem. Soc.* **126**, 14287-14296 (2004).
7. Nijhuis, C.A., Reus, W.F. & Whitesides, G.M. Molecular Rectification in Metal−SAM−Metal Oxide−Metal Junctions. *J. Am. Chem. Soc.* **131**, 17814-17827 (2009).
8. Yoon, H.J. *et al.* The Rate of Charge Tunneling through Self-Assembled Monolayers Is Insensitive to Many Functional Group Substitutions. *Angew. Chem. Int. Ed.* **51**, 4658-4661 (2012).

9. Tran, E., Grave, C., Whitesides, G.M. & Rampi, M.A. Controlling the electron transfer mechanism in metal–molecules–metal junctions. *Electrochim. Acta* **50**, 4850-4856 (2005).
10. McCreery, R.L. Molecular Electronic Junctions. *Chem. Mater.* **16**, 4477-4496 (2004).
11. Chen, F., Li, X., Hihath, J., Huang, Z. & Tao, N. Effect of Anchoring Groups on Single-Molecule Conductance: Comparative Study of Thiol-, Amine-, and Carboxylic-Acid-Terminated Molecules. *J. Am. Chem. Soc.* **128**, 15874-15881 (2006).
12. Park, Y.S. *et al.* Contact Chemistry and Single-Molecule Conductance: A Comparison of Phosphines, Methyl Sulfides, and Amines. *J. Am. Chem. Soc.* **129**, 15768-15769 (2007).
13. Cheng, Z.L. *et al.* In situ formation of highly conducting covalent Au-C contacts for single-molecule junctions. *Nat. Nanotechnol.* **6**, 353-357 (2011).
14. Li, Z., Smeu, M., Ratner, M.A. & Borguet, E. Effect of Anchoring Groups on Single Molecule Charge Transport through Porphyrins. *J. Phys. Chem. C* (2013).
15. Beebe, J.M., Engelkes, V.B., Miller, L.L. & Frisbie, C.D. Contact Resistance in Metal−Molecule−Metal Junctions Based on Aliphatic SAMs: Effects of Surface Linker and Metal Work Function. *J. Am. Chem. Soc.* **124**, 11268-11269 (2002).
16. Kim, B., Beebe, J.M., Jun, Y., Zhu, X.Y. & Frisbie, C.D. Correlation between HOMO Alignment and Contact Resistance in Molecular Junctions: Aromatic Thiols versus Aromatic Isocyanides. *J. Am. Chem. Soc.* **128**, 4970-4971 (2006).
17. Ahn, S. *et al.* Electronic transport and mechanical stability of carboxyl linked single-molecule junctions. *Phys. Chem. Chem. Phys.* **14**, 13841-13845 (2012).
18. Chiechi, R.C., Weiss, E.A., Dickey, M.D. & Whitesides, G.M. Eutectic Gallium–Indium (EGaIn): A Moldable Liquid Metal for Electrical Characterization of Self-Assembled Monolayers. *Angew. Chem. Int. Ed.* **47**, 142-144 (2008).
19. Nijhuis, C.A., Reus, W.F., Barber, J.R. & Whitesides, G.M. Comparison of SAM-Based Junctions with Ga_2O_3/EGaIn Top Electrodes to Other Large-Area Tunneling Junctions. *J. Phys. Chem. C* **116**, 14139-14150 (2012).
20. Weiss, E.A. *et al.* Si/SiO_2-Templated Formation of Ultraflat Metal Surfaces on Glass, Polymer, and Solder Supports: Their Use as Substrates for Self-Assembled Monolayers. *Langmuir* **23**, 9686-9694 (2007).
21. Simmons, J.G. Generalized Formula for the Electric Tunnel Effect between Similar Electrodes Separated by a Thin Insulating Film. *J. Appl. Phys.* **34**, 1793-1803 (1963).

22. Simmons, J.G. Electric Tunnel Effect between Dissimilar Electrodes Separated by a Thin Insulating Film. *J. Appl. Phys.* **34**, 2581-2590 (1963).
23. Akkerman, H.B. *et al.* Electron tunneling through alkanedithiol self-assembled monolayers in large-area molecular junctions. *PNAS* **104**, 11161-11166 (2007).
24. Cademartiri, L. *et al.* Electrical Resistance of Ag^{TS}–$S(CH_2)_n$−CH_3//Ga_2O_3/EGaIn Tunneling Junctions. *J. Phys. Chem. C* **116**, 10848-10860 (2012).
25. Fan, F.-R.F. *et al.* Charge Transport through Self-Assembled Monolayers of Compounds of Interest in Molecular Electronics. *J. Am. Chem. Soc.* **124**, 5550-5560 (2002).
26. Salomon, A. *et al.* Comparison of Electronic Transport Measurements on Organic Molecules. *Adv. Mater.* **15**, 1881-1890 (2003).
27. Diez-Perez, I. *et al.* Controlling single-molecule conductance through lateral coupling of π-orbitals. *Nat. Nanotechnol.* **6**, 226-231 (2011).
28. Guedon, C.M. *et al.* Observation of quantum interference in molecular charge transport. *Nat. Nanotechnol.* **7**, 305-309 (2012).
29. Aradhya, S.V. & Venkataraman, L. Single-molecule junctions beyond electronic transport. *Nat. Nanotechnol.* **8**, 399-410 (2013).
30. Tao, Y.T. Structural comparison of self-assembled monolayers of n-alkanoic acids on the surfaces of silver, copper, and aluminum. *J. Am. Chem. Soc.* **115**, 4350-4358 (1993).
31. Tao, Y.-T., Hietpas, G.D. & Allara, D.L. HCl Vapor-Induced Structural Rearrangements of n-Alkanoate Self-Assembled Monolayers on Ambient Silver, Copper, and Aluminum Surfaces. *J. Am. Chem. Soc.* **118**, 6724-6735 (1996).
32. Lin, S.-Y. *et al.* Structures of Self-Assembled Monolayers of n-Alkanoic Acids on Gold Surfaces Modified by Underpotential Deposition of Silver and Copper: Odd−Even Effect. *Langmuir* **18**, 5473-5478 (2002).
33. Hsu, M.-H. *et al.* H2S-Induced Reorganization of Mixed Monolayer of Carboxylic Derivatives on Silver Surface. *Langmuir* **20**, 3641-3647 (2004).
34. Kawasaki, M. & Iino, M. Self-Assembly of Alkanethiol Monolayers on Ag−Au(111) Alloy Surfaces. *J. Phys. Chem. B* **110**, 21124-21130 (2006).
35. Schlotter, N.E., Porter, M.D., Bright, T.B. & Allara, D.L. Formation and Structure of a Spontaneously Adsorbed Monolayer of Arachidic on Silver. *Chem. Phys. Lett.* **132**, 93-98 (1986).

36. Simeone, F.C. *et al.* Defining Injection Current and Effective Contact Area for EGaIn-based Molecular Tunnel Junctions. *Submitted* (2013).
37. Kristensen, I.S., Mowbray, D.J., Thygesen, K.S. & Jacobsen, K.W. Comparative study of anchoring groups for molecular electronics: structure and conductance of Au–S–Au and Au–NH_2–Au junctions. *J. Phys. Condens. Matter* **20**, 374101 (2008).
38. Santiago, M. *et al.* Adverse effects of asymmetric contacts on single molecule conductances of $HS(CH_2)_nCOOH$ in nanoelectrical junctions. *Nanotechnol.* **20**, 125203 (2009).
39. Tsutsui, M., Taniguchi, M. & Kawai, T. Quantitative Evaluation of Metal−Molecule Contact Stability at the Single-Molecule Level. *J. Am. Chem. Soc.* **131**, 10552-10556 (2009).
40. Hong, W. *et al.* Single Molecular Conductance of Tolanes: Experimental and Theoretical Study on the Junction Evolution Dependent on the Anchoring Group. *J. Am. Chem. Soc.* **134**, 2292-2304 (2011).
41. Zimbovskaya, N.A. & Pederson, M.R. Electron transport through molecular junctions. *Phys. Rep.* **509**, 1-87 (2011).
42. Chu, C., Na, J.-S. & Parsons, G.N. Conductivity in Alkylamine/Gold and Alkanethiol/Gold Molecular Junctions Measured in Molecule/Nanoparticle/Molecule Bridges and Conducting Probe Structures. *J. Am. Chem. Soc.* **129**, 2287-2296 (2007).
43. Tao, Y.T., Lee, M.T. & Chang, S.C. Effect of biphenyl and naphthyl groups on the structure of self-assembled monolayers: packing, orientation, and wetting properties. *J. Am. Chem. Soc.* **115**, 9547-9555 (1993).
44. Holmlin, R.E. *et al.* Electron Transport through Thin Organic Films in Metal−Insulator−Metal Junctions Based on Self-Assembled Monolayers. *J. Am. Chem. Soc.* **123**, 5075-5085 (2001).
45. Fracasso, D., Muglali, M.I., Rohwerder, M., Terfort, A. & Chiechi, R.C. Influence of an Atom in EGaIn/Ga_2O_3 Tunneling Junctions Comprising Self-Assembled Monolayers. *J. Phys. Chem. C* **117**, 11367-11376 (2013).
46. Salomon, A., Shpaisman, H., Seitz, O., Boecking, T. & Cahen, D. Temperature-Dependent Electronic Transport through Alkyl Chain Monolayers: Evidence for a Molecular Signature. *J. Phys. Chem. C* **112**, 3969-3974 (2008).

47. Levine, I. *et al.* Molecular Length, Monolayer Density, and Charge Transport: Lessons from Al–AlO_x/Alkyl–Phosphonate/Hg Junctions. *Langmuir* **28**, 404-415 (2011).
48. Wang, G., Kim, T.-W. & Lee, T. Electrical transport characteristics through molecular layers. *J. Mater. Chem.* **21**, 18117-18136 (2011).

Acknowledgements

We thank Dr. Mathieu Gonidec for his technical contribution. This work was supported by a subcontract from Northwestern University from the Department of Energy (DE-SC0000989) on materials and measurements of charge transport.

Author contributions

K.-C.L. and G.M.W. conceived this project. K.-C.L. performed the experiments of carboxylates; F.C.S. performed the experiments of *n*-alkanethiolates. All authors analysed the junction measurements, discussed the results, and contributed to the manuscript.

Additional Information

Supplementary information including Table S1 is available in the online version of the paper. Reprints and permissions information is available online at www.nature.com/reprints. Correspondence and requests for materials should be addressed to G.M.W.

Competing financial interests

The authors declare no competing financial interests.

Figure 1. a, A cartoon representation of the $Ag^{TS}XR//Ga_2O_3/EGaIn$ junction (X = $–SCH_2–$ and $–O_2C–$); **b**, log-current density (log|*J*|) *versus* bias (*V*) plots for the $Ag^{TS}O_2C(CH_2)_nCH_3//Ga_2O_3/EGaIn$ junctions with various chain lengths (4 to 18 carbons including the top methyl group and the bottom anchoring group), as indicated in the figure; **c**, a plot of log-current density (log|*J*|) against the chain length of *n*-alkanoates (including the terminal C–H bond), given in number of carbons at -0.5 V. The linear-least square fits for *n*-alkanoates (dotted line) and for *n*-alkanethiolates (solid line) and the results of electrical measurement are inserted in the figure.

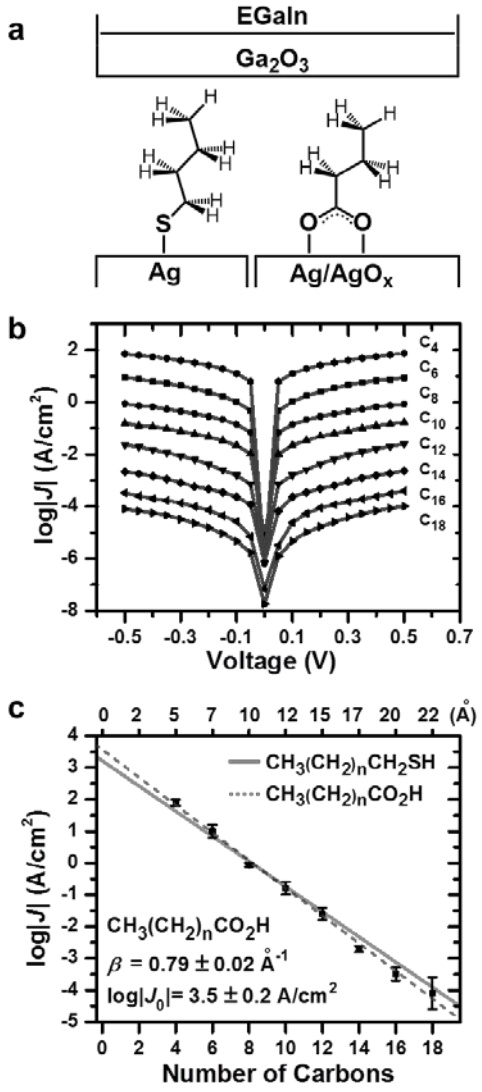

Figure 2. Histograms for values of log|*J*| data derived from *n*-alkanoates at -0.5 V. Each histogram is fitted with a Gaussian curve (black curve).

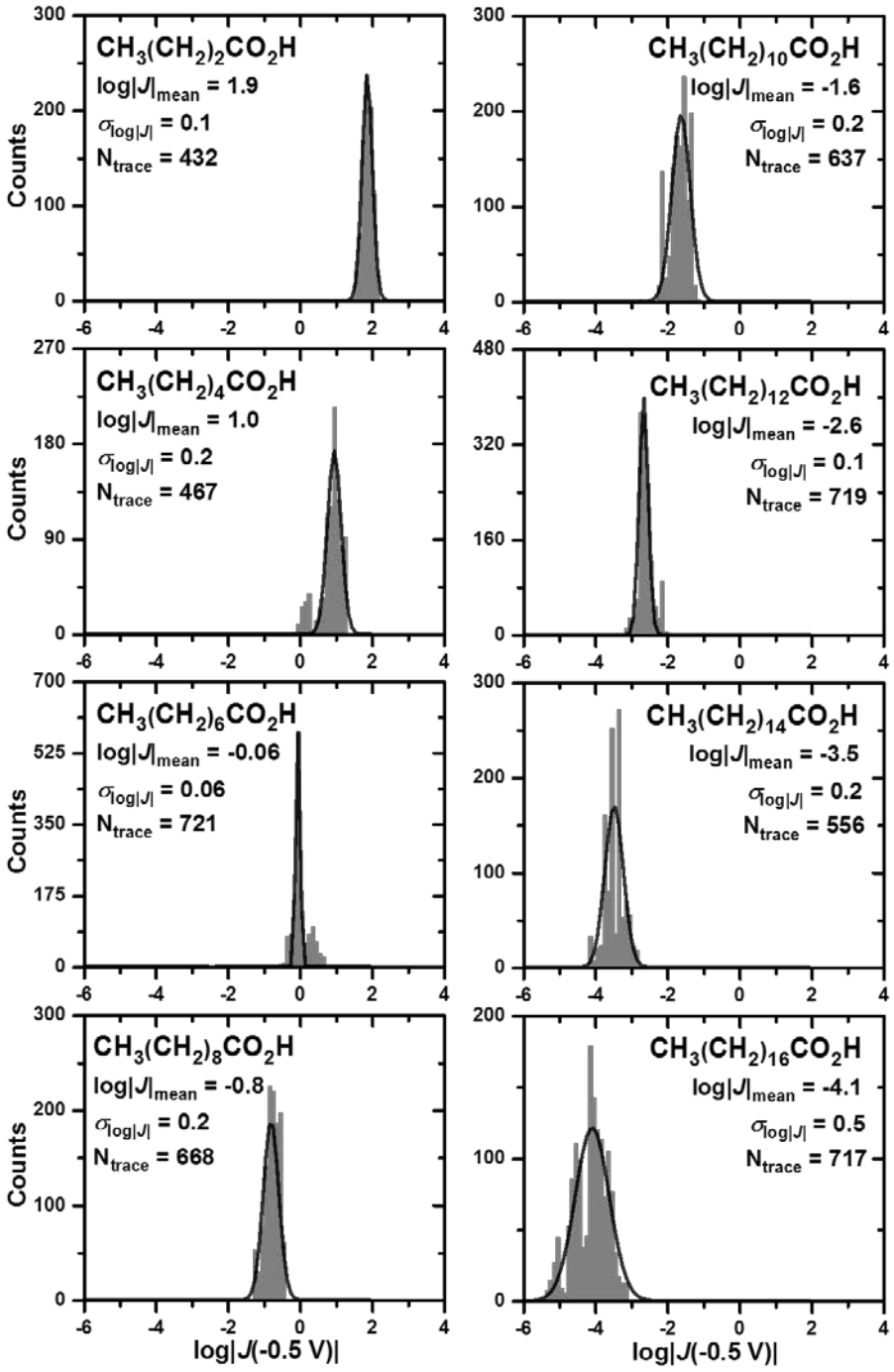

Figure 3. a, A cartoon representation of the junction structure comprising oligo(phenylene)-carboxylate SAMs. The carboxylate forms a bidentate coordination to the surface of Ag; b, a plot of log-current density (log|*J*|) against the calculated length (Å), including the terminal C–H bond, of oligo(phenylene)carboxylates, given in the number of phenylene units at -0.5 V. The linear-least square fits (dotted line) and the results of electrical measurement are inserted in the figure.

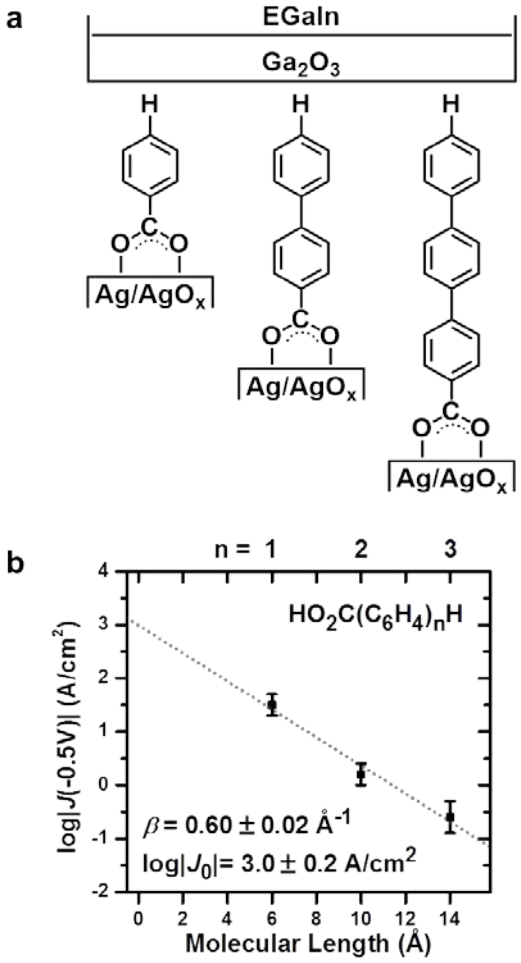

Figure 4. Histograms of log|*J*| for **a**, benzoate; **b**, biphenyl-4-carboxylate; and **c**, *p*-terphenyl-4-carboxylate in the $Ag^{TS}O_2C(C_6H_4)_nH//Ga_2O_3/EGaIn$ junctions (n= 1 – 3) at -0.5 V. Each histogram is fitted with a Gaussian curve (black curve).

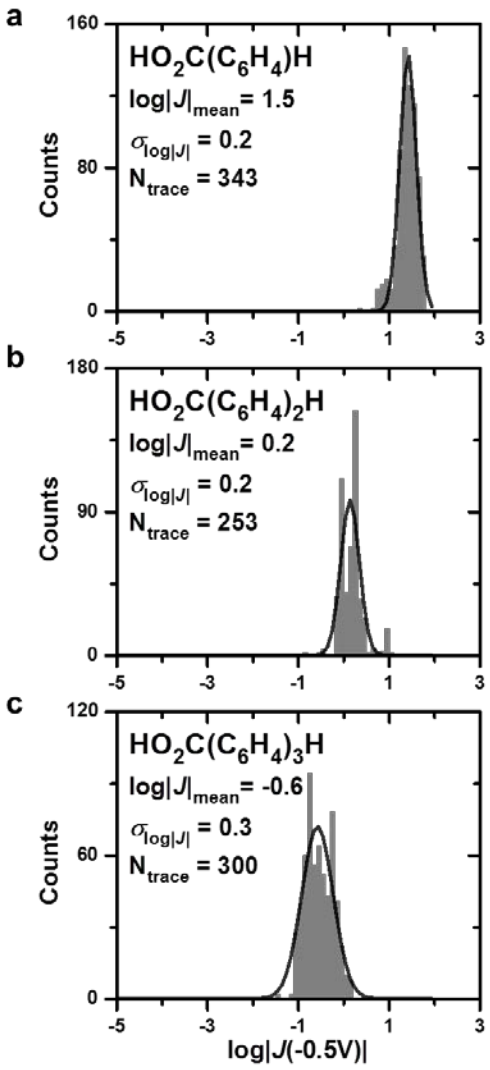

Table 1. Summary of data derived from *n*-alkanoates (C_nO_2) and *n*-alkanethiolates[36] (C_nS) at -0.5 V to illustrate the similarity in the charge transport characteristics among the two homologous SAMs.

***n*-alkanoates**							***n*-alkanethiolates**	
C_nO_2	Number of Samples	Working Junctions	Yield (%)	traces	$\log\|J\|_{median}$ (A/cm^2)	$\log\|J\|_{mean} \pm \sigma_{log}$ (A/cm^2)	**C_nS**	$\log\|J\|_{mean} \pm \sigma_{log}$ (A/cm^2)
C_4O_2	3	20	95	432	1.85	1.9 ± 0.10	C_4S	1.6 ± 0.5
C_6O_2	3	20	90	467	0.95	1.0 ± 0.20	C_6S	0.9 ± 0.3
C_8O_2	4	30	97	721	-0.05	-0.06 ± 0.06	C_8S	0.2 ± 0.3
$C_{10}O_2$	4	29	91	668	-0.85	-0.8 ± 0.20	$C_{10}S$	-1.1 ± 0.3
$C_{12}O_2$	3	27	90	637	-1.65	-1.6 ± 0.20	$C_{12}S$	-1.5 ± 0.5
$C_{14}O_2$	4	32	97	719	-2.65	-2.7 ± 0.10	$C_{14}S$	-2.2 ± 0.3
$C_{16}O_2$	3	24	91	556	-3.55	-3.5 ± 0.20	$C_{16}S$	-3.2 ± 0.3
$C_{18}O_2$	4	32	84	717	-4.15	-4.1 ± 0.50	$C_{18}S$	-3.9 ± 0.3
C_0O_2						-3.5 ± 0.20 **($\log\|J_0\|$)** β = 0.79 ± 0.02 $Å^{-1}$	**C_0S**	**3.2 ± 0.3 ($\log\|J_0\|$)** β = 0.75 ± 0.02 $Å^{-1}$

Table 2. Summary of data derived from oligo(phenylene)carboxylates (Ag^{TS}–O_2C–$(C_6H_4)_nH$//Ga_2O_3/EGaIn, n = 1 – 3) at -0.5 V.

Oligo(phenylene)carboxylates							
n	Molecular Lengths (Å)	Number of Samples	Working Junctions	Yield (%)	traces	$\log\|J\|_{median}$ (A/cm^2)	$\log\|J\|_{mean} \pm \sigma_{log}$ (A/cm^2)
1	6	3	18	72	343	1.45	1.5 ± 0.2
2	10	3	12	80	253	0.15	0.2 ± 0.2
3	14	3	15	79	300	-0.55	-0.6 ± 0.3
C_0O_2							**3.0 ± 0.2 ($\log\|J_0\|$)**
							β = 0.60 ± 0.02 $Å^{-1}$

Graphical Abstract

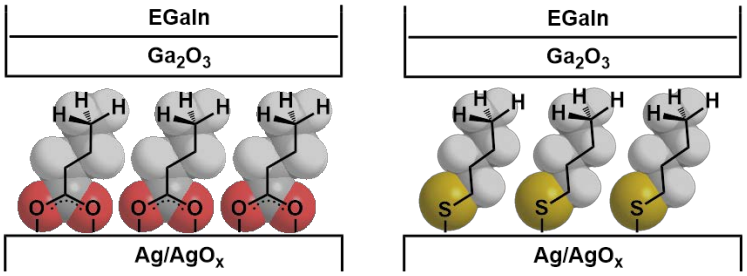

This manuscript describes a comparative study on the role of the metal–SAM interface in the charge tunneling process. We investigate the rate of charge transport through EGaIn-based junctions comprising self-assembled monolayers (SAMs) of organo-thiolates and carboxylates.